

Measurement and Simulation of Striae in Optical Glass

H. Gross^a, M. Hofmann^b, R. Jedamzik^c, P. Hartmann^c, S. Sinzinger^d

^aCarl Zeiss AG, Central R&D, Optical Design, 73446 Oberkochen, Germany, ^bDILAS Diodenlaser GmbH, 55129 Mainz-Hechtsheim, Germany, ^cSchott AG, Hattenbergstr 10, 55122 Mainz, Germany,

^dTechnische Universität Ilmenau, Technische Optik, P.O. Box 100565, 98684 Ilmenau, Germany
<mailto:gross@zeiss.de>

ABSTRACT

One of the most important properties of optical glass is the excellent spatial homogeneity of the refractive index of the material. Nevertheless, sometimes spatially short-range inhomogeneities are formed during the production process. These striae are strongly anisotropic due to the process of glass melting. In optical systems, they cause degradation of the performance with a complicated behavior. The quality specification of the glass homogeneity usually is given by simple values of phase differences along the main propagation direction of the light in an area of a certain size. For the measurement of these effects, interferometry can be used, which is a quite expensive method in reality. The observation of striae shadowgraph pictures is a faster and more frequently used method. The evaluation and quantitative reconstruction of the inhomogeneities in glass based on the striae technique are the main goal of this work. We revise the experimental setup and develop models to simulate the measurements for thin and thick samples. The results of the shadowgraph method are compared with interferometric measurements. A more refined evaluation which is not only based on the image contrast allows a unique and accurate reconstruction of the size and the phase height of striae with negligible axial extension. A simple procedure shows how one can estimate the effect in thick samples in practice approximately.

Keywords: Striae, homogeneity, Schlieren, shadowgraphy

1. INTRODUCTION

The characterization, measurement and simulation of striae in optical glass is investigated for a long time^[1]. The contribution to this topic presented here is mainly based on the work in^[2]. The quality of the optical glass in lenses and other components is an important property for the performance of optical systems. Therefore a number of criteria is defined to prescribe the parameters of optical glass properly. The major data are the absolute value of the index of refraction and the dispersion of the glass for the desired wavelength range. The homogeneity of the refractive index in the whole volume of a sample is an additional property, which must be considered. These properties of a sample are therefore considered in special standardization procedures^{[3][4][5]}. In the ISO document^[3], the tolerance of inhomogeneity is defined by two values. First a maximum permissible variation of the refractive index within an uncertainty of better than 10^{-6} is considered. There are 6 classes, which allow values from $0.5 \cdot 10^{-6}$ to $50 \cdot 10^{-6}$ for the differences in the refractive index. Secondly the density of the area perturbed by striae is divided into 5 classes from extremely free samples to samples with 10% of the cross-section area covered by corresponding phase differences. The military norm^[4] and an internally used characterization of the glass vendor Schott defines four degrees of strength of striae according to types A to D with phase differences from 10 nm to 60 nm^[6]. From experience one knows that the delivery quality of C-grade and much better striae is very conservative. So there is a need for an improved striae specification avoiding losses due to overspecification. However, such revision presupposes a better measurement method and more knowledge about the effects of striae in optical system performance. This work concentrates on the improvement of the measurement method.

There are three prominent measuring techniques for material inhomogeneities, which are proposed in the literature. The classical Töpler Schlieren darkfield method is one possibility^{[1][7][8]}. A second method, which is quite fast and easy is the production of a shadow image through the sample glass block^{[7][9]}. Figure 1 shows a shadowgraph image of a glass sample with the characteristic striated geometry. An additional possibility is the interferometric characterization. This method provides precise quantitative results of the phase delays resulting from internal striae. Usually a collimated beam is chosen to illuminate the sample with perpendicular incidence at the entrance and the exit surface. An immersion fluid

can be used in order to compensate for surface roughness. Otherwise, if the test sample is located in air, the surfaces must be polished to optical quality to avoid artifacts from the surfaces. Figure 2 shows a typical image of an interferogram of a perturbed glass sample. The shadow image method is the preferred measuring technique, because the setup is simple, robust and can be used in the environment of the optical shop without problems.

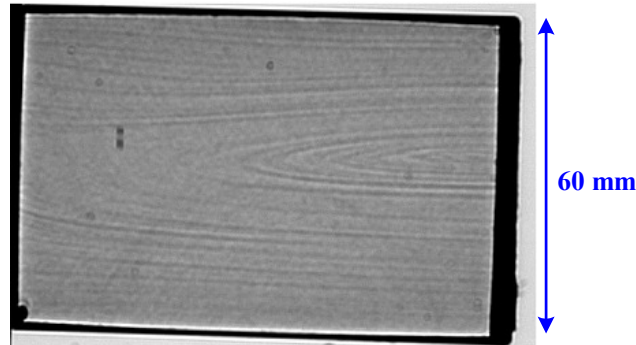


Fig. 1. Typical structure of the shadowgraph image for a sample of optical glass.

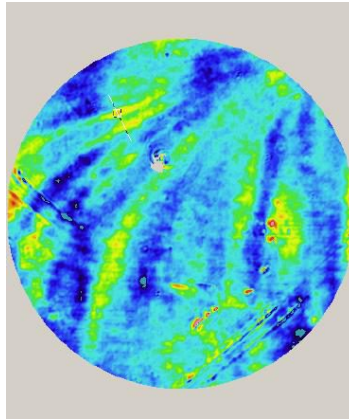


Fig. 2. Interferogram of a glass sample. Some scratches and perturbations on the sample surface can be seen.

Refractive index perturbations perpendicular to the optical axis influence the optical systems quality quite heavily. There are several investigations in the literature concerning the effect of material inhomogeneities on image quality^{[10]-[13]}. These calculations need quantitative data for geometry and size of the striae perturbations. This work presents a simple procedure for extracting such data in an approximate way from shadowgraph measurements.

2. MEASUREMENT SETUP

The classical setup of a shadowgraph measuring arrangement is shown in figure 3^{[7][9]}. The light of a mercury arc lamp with a small luminous area illuminates the sample without further beam shaping components. The light cone transmitting the sample is nearly collimated due to a large distance. The shadow image of the transmitted light is projected onto a distant screen. This image is recorded with a camera. The sample is arranged on a turntable in order to allow slight adjustments along the vertical axes and to choose the orientation of the striae relative to the illumination. A typical image from a glass sample with striae is shown in figure 1.

One of the major problems in interpreting the shadow images is the quantitative calibration and evaluation. For this purpose, a test plate can be used, which contains a matrix of small slits with well defined widths and phase steps^[14]. Figure 4 shows a part of the image of this two-dimensional test plate for illustration. Every phase slit generates a separate diffraction pattern on the screen, which can be evaluated, e.g. by comparison of the structure and contrast of the fringes. However it has to be kept in mind, that this plate is a two-dimensional simplified model of a three-dimensional glass sample.

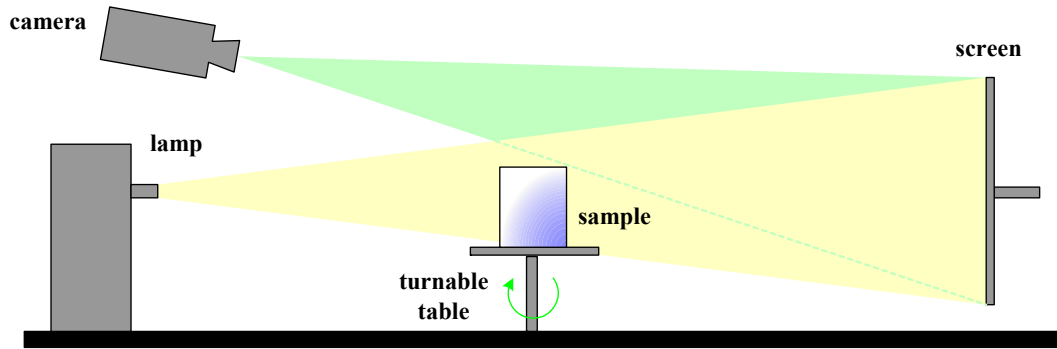


Fig. 3. Experimental setup for the striae test used for the shadowgraph image method.

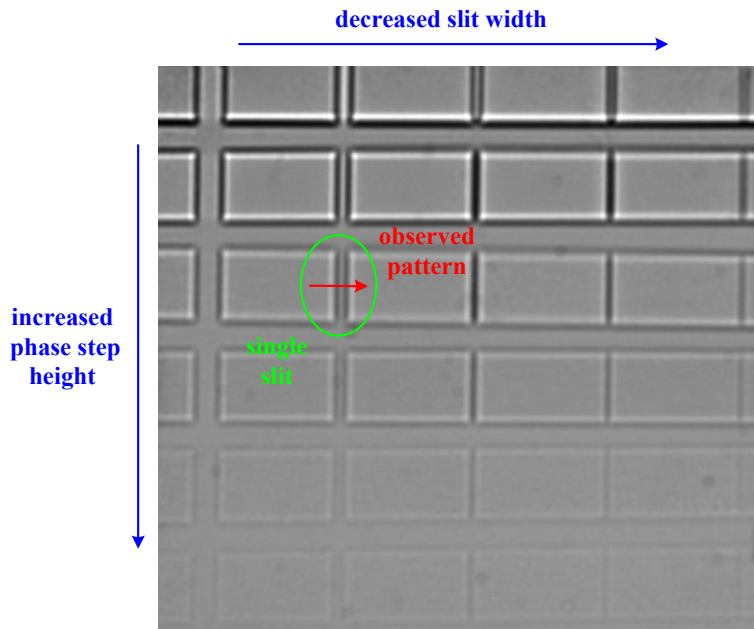


Fig. 4. Test plate with a matrix of defined slits of variable width with different phase steps.

3. MODELLING THE EXPERIMENT

We use a diffraction based simulation model in order to gain a full understanding of the shadowgraph imaging method and a quantitative evaluation of the recorded images with the goal to reconstruct the refractive index inhomogeneity. There are two different possibilities to model the sample itself. In a simplified model, the effect of the sample is considered as a thin sheet phase mask. This scheme is sketched in the upper picture a) of figure 5. To get a more detailed understanding, if the diffraction effects inside a thick sample must be considered or can be neglected, a more refined model is used to describe the light propagation inside the glass block accurately. This attempt corresponds to the lower picture b) in figure 5.

In the most general approach, the light from the lamp is partially coherent and the spectral bandwidth and the finite size of the radiating area must be taken into account. According to the well-known source integration concept, all computations can be obtained as a superpositions of elementary contributions of monochromatic point sources. Therefore coherent beam propagation is the basic task in the simulation of the setup. In figure 5, the complex fields E_1 to E_4 are indicated at the various positions of the arrangement. A point source is assumed for the field E_1 at the lamp. There are three steps necessary to get the desired field strength E_4 on the screen. From the viewpoint of diffraction calculation, different propagators must be used for the three transfers.

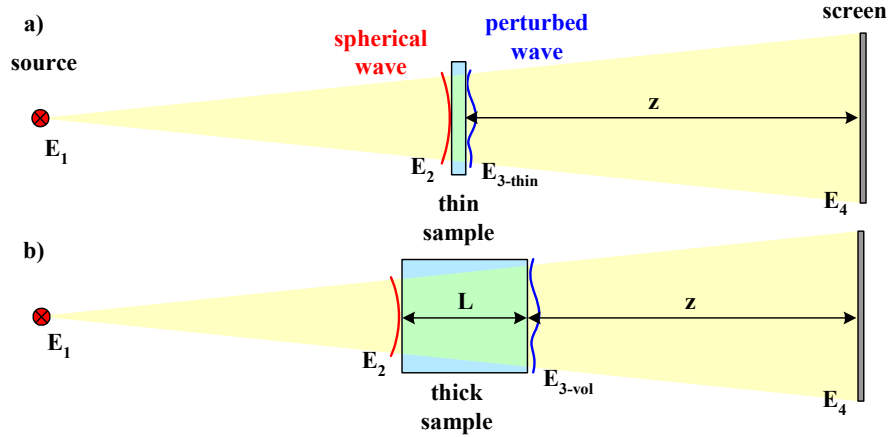


Fig. 5. In a) a two-dimensional sample model is shown with a thin sheet. Transverse changes of the field inside the volume are neglected here. In b) a more general model incorporates the volume effects of propagation inside the sample. The fields E_j indicate the different steps of the calculation.

The field E_2 in front of the sample can be considered as a spherical wave with constant amplitude for all transverse coordinates x, y . In the case of the thin sheet model (figure 5a), the modification of the field by the sample is quite easy and can be described by the equation

$$E_{3-thin}(x, y) = E_2(x, y) \cdot e^{2\pi i W(x, y)} \quad (1)$$

Here $W(x, y)$ represents the phase mask, which describes the effect of the index changes in the probe integrated along the optical axis. The transfer of the field from the sample position to the observation screen is calculated by a diffraction integral in Fresnel approximation^[15]

$$E_4(x, y) = C \cdot \iint E_3(x', y') \cdot e^{-\frac{i\pi}{\lambda z} [(x'-x)^2 + (y'-y)^2]} dx' dy' \quad (2)$$

Since the camera can only detect intensities, the phase information of the complex field is lost here. Therefore additional phase factors in the diffraction integral are omitted here for simplicity. In the case of the more sophisticated model of a volume sample, the field E_{3-vol} is computed via a finite difference split step propagation method along the axial extension L of the sample^[15]. The length L typically has a size between 20 mm and 50 mm, the distances from the sample to the source and the screen are in the range of 1 m. A two-dimensional ADI-formalism solves the Helmholtz wave equation by a discretization of the derivatives according to the Douglas scheme. The resulting tridiagonal linear system of equations is solved by using the well-known Thomas algorithm. In comparison to the thin sheet calculation model, this is a time consuming procedure. For a typical sampling of 512x512 transverse and 200 axial sample points the computation of one source point typically takes two minutes of time on a conventional computer. The integration over the extension of the source and the superposition of all wavelengths of the spectrum of the lamp results in approximately two hours computation time for one image for typical circumstances.

4. COMPARISON OF THEORY AND EXPERIMENT

To verify the simulation model, first the results of the interferometric measurements, the shadowgraph images and the simulations are compared. For this purpose, the phase map of the interferometric measurement of a specific sample is imported into the simulation software. With this empirical function, the shadow image is calculated. This picture is compared with the experimentally recorded image. An excellent agreement is obtained for this comparison.

In a second test, the diffraction images of the calibrated test plate are compared with calculated images for the same properties of the phase slit. This comparison is performed for the cross sections perpendicular to the slit direction. The results strongly depend on the accurate model of the light source. Figure 6 shows some diffraction patterns resulting from the simulation, in the upper row for a monochromatic point source, a polychromatic point source and a polychromatic extended area light source respectively. In the lower row, two experimental results are shown, where an

extended light source was used which was filtered to quasi-monochromatic performance or used as a broad spectral light source. Only the right column with the general case is really comparable and an excellent agreement is recognized between simulation and experiment. It can be seen, that the spectral width as well as the extension of the radiating area of the source play an essential role and have to be taken into account. The contrast of the major peak is nearly constant in all the three simulated cases, but the modulation of the side lobes is significantly reduced, if the source extension and the broad spectrum are taken into account. This shows that it is necessary to use the general light source model to get quantitatively correct results. This option is used in all the calculation results below.

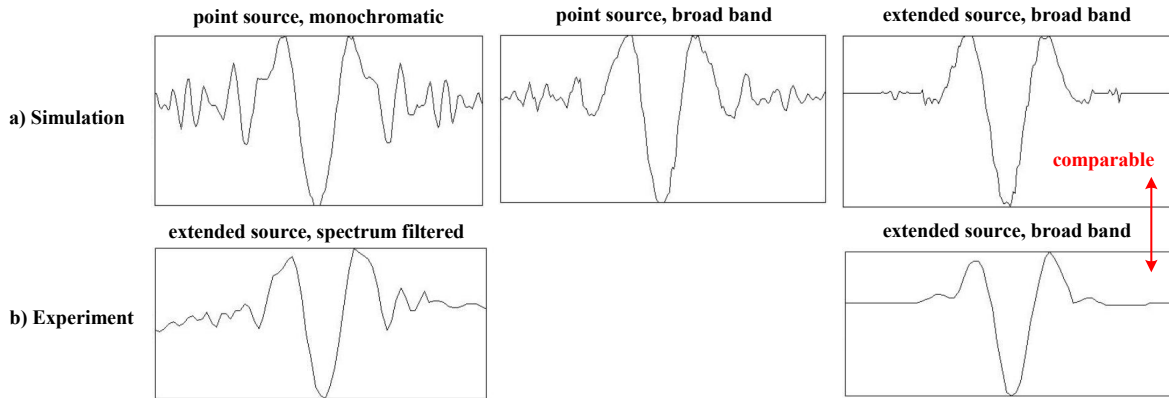


Fig. 6. Diffraction pattern of a single slit with width of 0.5 mm and phase step height of 30 nm in the simulation a) and the experiment b). The influence of the spectral characteristic and the extension of the source is clearly seen. The last column corresponds to the general case and shows a good agreement between theory and experiment. All diagrams have the same scales.

If the length of the samples is smaller than 100 mm, which is a typically the case, the simulation with the two propagation models described above show comparable results. Therefore one may conclude, that under these circumstances the volume effects are negligible and the thin sheet model gives a sufficiently detailed description of the setup.

5. QUANTITATIVE RECONSTRUCTION OF THE INDEX DISTRIBUTION

Several attempts to get quantitative data from corresponding measurements of striae are reported in the literature. Mostly, these investigations assume quite simple geometries for the inhomogeneities^[16]. The goal of this work is a quantitative reconstruction of the phase strips occurring in practice due to the striae distribution in a glass sample. With the values for the width and the phase height of such a perturbation, a tolerance calculation can be performed to check the usability of the glass sample. In the well known specification standard ISO 10110 part 4^[3], only the optical path difference is used to define the homogeneity tolerance of a sample, which is usually determined with the shadowgraph method, however only in comparison to reference samples. The attempts to standardize the shadowgraph method failed since many years because of the absence of an objective and reproducible phase step measurement method with high spatial resolution or at least a calibration and comparison procedure for the shadow images. The presented work is meant as a significant step towards such procedure. Several times the use of a reference plate with artificial phase steps were proposed. But in the end it was found that the simple phase step approach considering the contrast only was not sufficient for the following reason.

If the image data of the test plate are analyzed and the dependence of the contrast on the slit width and the phase height is determined, one gets the representation of figure 7. Larger phase steps usually create larger contrast values. The dependence of the contrast for different values of the slit width shows a maximum for medium values of approximately 0.5 mm and hence there is no one-to-one correlation. If a contrast value is extracted from measured data, the corresponding width of the perturbation cannot be evaluated unambiguously. For example the ranges indicated by the ellipses cannot be distinguished.

To get a unique reconstruction recipe, an additional measurement is needed. By carefully examining the diffraction patterns of the test chart, it can be seen, that there is an additional property, which allows discriminating different slit widths and phase step heights. If a one-dimensional Fourier transform is performed on the diffraction pattern in the

direction across the slit, a typical picture is obtained. Figure 8 shows the power spectral density of a pattern for illustration. The spectrum smoothly changes its shape if the parameters of the slit are modified, but the overall character of the curve remains constant. If the dependence of the first minimum position is considered as a function of the slit width, a nearly linear relationship is obtained. This enables a discrimination of the ambiguous regions of figure 7.

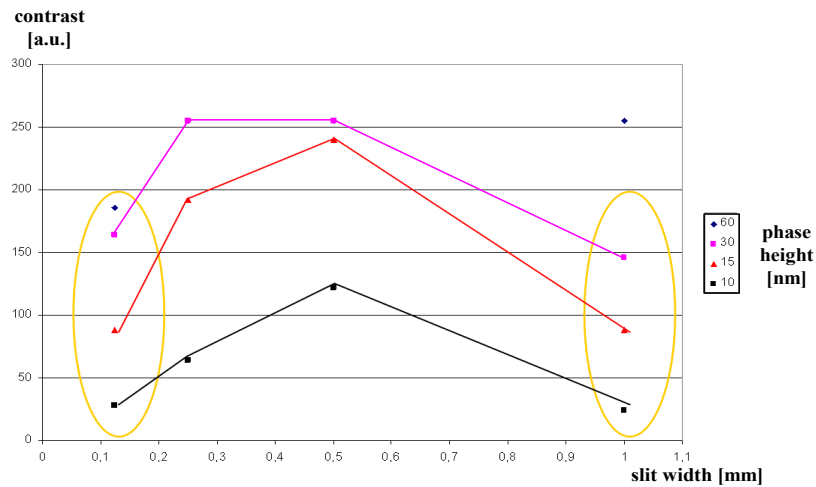


Fig. 7. Contrast of the shadow image as a function of the slit width for different values of the phase step height in the experiment.

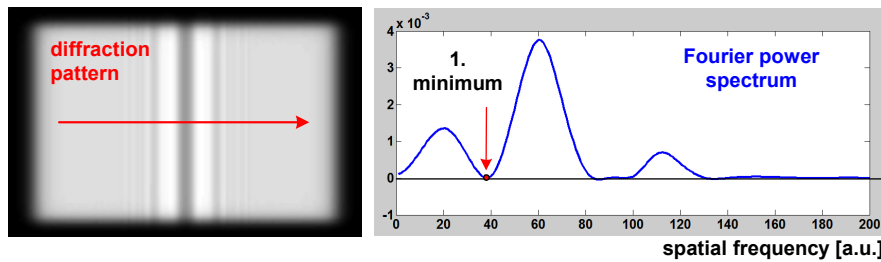


Fig. 8. Fourier power spectrum of a cross section of a calculated diffraction pattern of a slit with a phase step.

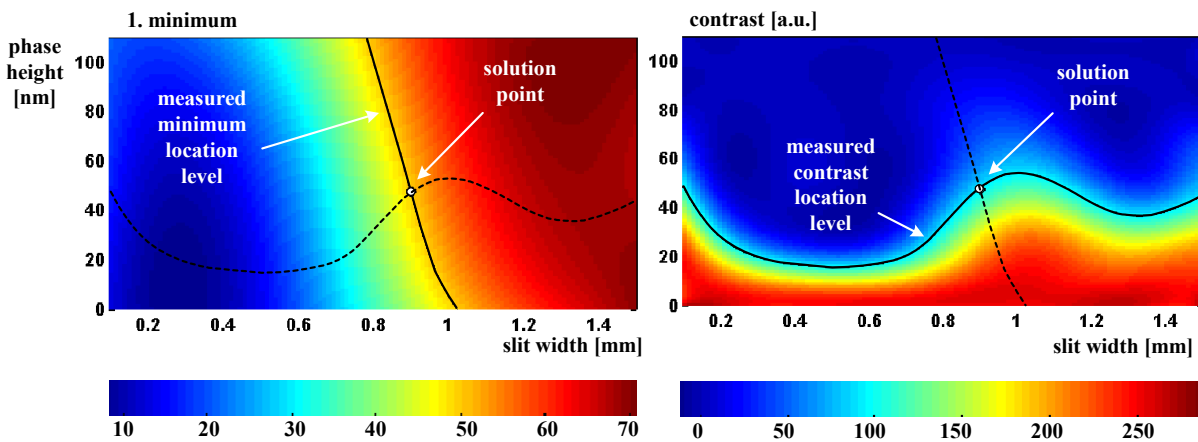


Fig. 9. Reconstruction of the phase height and the slit width from measured data of the contrast and the position of the first minimum of the Fourier spectrum.

The left part of figure 9 shows the dependence of the spatial frequency of the first minimum of the power spectral density on the slit width and the phase height. This two-dimensional function approximately has the behavior of a tilted linear ramp for medium sized perturbation widths. If in addition the contrast dependence is represented in a similar way,

the right picture of figure 9 is obtained. This representation clearly shows the ambiguity of the evaluation of the contrast data only.

If now an image is given, it is easily possible to analyze the contrast of the diffraction pattern and to determine the first minimum of its power spectrum. The corresponding contour curves for an example are indicated in the figure by solid black lines. The intersection of both curves allows determining the width and the phase height in an unambiguous way. Alternatively it is possible to find the solution point in a two-dimensional merit function with a standard least square procedure. In the practical calibration, the available points of measured data from the test plate are fitted with a two-dimensional set of Legendre polynomials^[15] to get smooth representations of the functions. Therefore the evaluation of the diffraction pattern of the shadow image must be analyzed to extract the contrast and the spatial frequency of the minimum in the Fourier spectrum to get a quantitative reconstruction of the slit parameter. This procedure works well for an isolated pattern in the image. If a complete image has to be analyzed with a complicated superposition of various diffraction patterns of several layers of striae, this evaluation provides at least a good estimation.

6. THICK SAMPLES

If the considered sample is thick, the approximation of a thin sheet and a reduction of the ray deviation into a single plane seems to be no longer possible, the quantitative reconstruction of the refractive index distribution is much more complicated. In general, a complete tomographic measurement with a variation of the inclination angle is an option. Since the effect of the outer surfaces has an essential influence in this case and many single tilt positions must be evaluated, this kind of measurement is very time consuming and complicated. Therefore, this method is only used in very special cases and is not feasible in the practical optical shop testing procedure. If the behavior of the striae geometry is analyzed carefully, it is seen, that there is mostly a layered structure of index variations found. This can be explained by the glass production process. Striae are mainly generated due to the unfinished mixing of the raw materials during melting. Homogenization during the melting process takes place due to convection processes in the tank and in the refining chamber. An additional mixing process within the mixing chamber smoothens out the inhomogeneities further. Again figure 1 illustrates the corresponding geometry.

If the light propagation is oriented perpendicular to the layers and they are assumed to be plane for simplicity, there is nearly no influence seen on the ray path. If the ray path goes parallel to the layers, every layer approximately acts as a phase slit and a considerable deviation of the rays is obtained. If now the sample is rotated, the various phase delays along the ray path are averaged and in summary, nearly no difference occurs between neighboring rays. Figure 10 illustrates this simple picture.

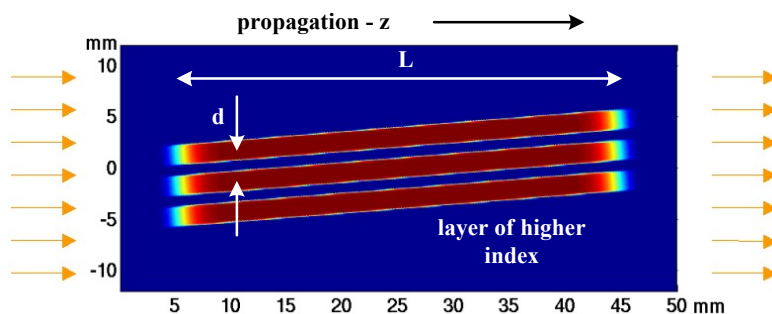


Fig. 10. Schematic illustration of the typical layered geometry of striae in optical glass.

If L is the length of the layers and d their distance, the contrast should vanish due to this averaging of phase differences for a tilt angle of approximately

$$\tan \varphi = \frac{d}{L} \quad (3)$$

Figure 11 shows for example the striae effect in a small part of a sample as an interferogram and as a shadow image. The five rows of pictures correspond to different rotation angles of the sample relative to the direction of the light

propagation. It can be seen, that the contrast of the images is reduced with growing angles as expected in both types of measurements. The zero angle orientation corresponds to a light propagation along the layer direction.

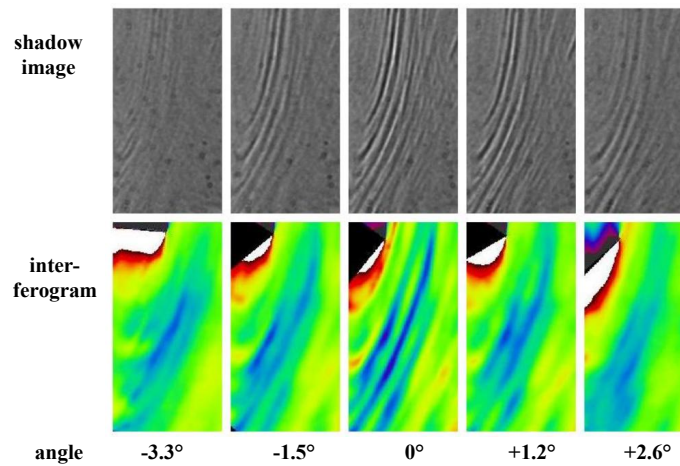


Fig. 11. Interferogram and shadow image of a sample with layered striae for five different tilt angles.

If a single striae strip is considered, the change of the contrast as a function of the rotation angle φ can be evaluated quantitatively. This is shown in figure 12, where the left part shows three distinct shadow images, in the graph on the right side the contrast is indicated as a function of the rotation angle. The contrast vanishes in this example for a tilt angle of approximately 2.5° relative to the centered position. With the thickness of the glass sample of 30 mm in this case the distance between two neighboring layers can be estimated with the help of equation (3) to 1.3 mm.

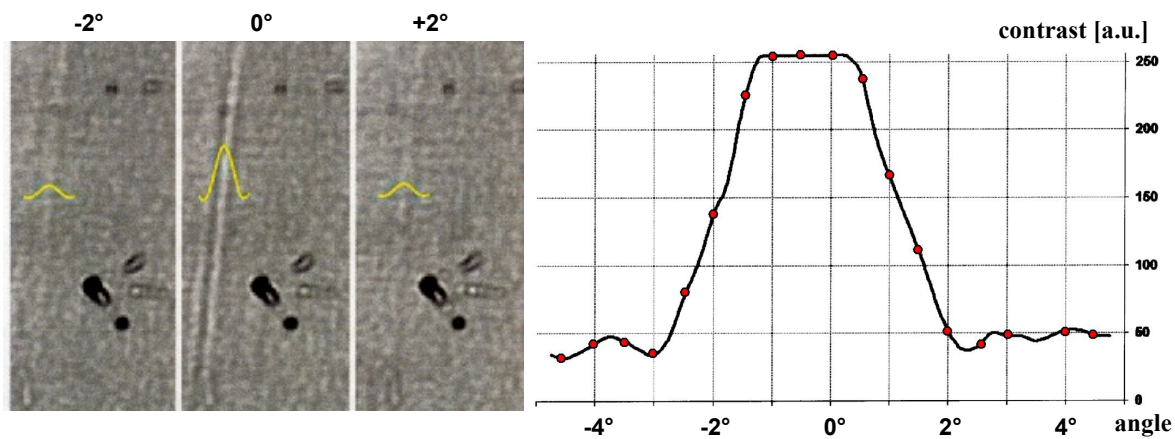


Fig. 12. Reduction of the shadow image contrast by tilting the sample for a special single striae. In this case, the contrast breaks down, if the sample is rotated by approximately $\pm 2.5^\circ$.

7. SUMMARY

It is shown that the structure of glass striae inhomogeneities has the typical geometry of a layered structure due to the glass melting process. The largest effect of these perturbations on the transmitted light is obtained, if the rays are oriented parallel to the layers. In this case a single striae layer acts approximately as a phase bump of a characteristic width and phase height. The results of interferometric measurements, shadowgraph images and simulations show a good agreement. In a first approximation, it is possible to neglect the volume effects and to describe the sample by a thin sheet model. A quantitative reconstruction of the two parameters to characterize the striae is possible with the help of the diffraction image. If the contrast and the power spectrum density are used for the evaluation, the determination of the parameters is unique. The use of the contrast alone is not sufficient to get clear results. In thick samples, a variation of

the ray orientation relative to the layer direction allows one to maximize the contrast. In this arrangement, the decrease of the contrast with the tilt angle allows a rough estimation of the ratio between width and length of the layer. A general reconstruction of the three-dimensional distribution of the refractive index is costly and requires a full tomographic measurement.

REFERENCES

- [1] J. R. Meyer-Arendt (Ed.), "Selected Papers on Schlieren Optics", SPIE Milestone Series, Vol. MS 61, SPIE Press, Bellingham (1992)
- [2] M. Hofmann, "Simulation von Schlieren in optischem Glas", M.Sc. thesis, Technische Universität Ilmenau, 2008
- [3] International standard ISO 10110-4, "Optics and optical instruments - Preparation of drawings for optical elements and systems", Part 4. "Inhomogeneity and Striae", (1997)
- [4] "Military specification, glass, optical", MIL-G-174B, U.S. Dept. of Defense (1986)
- [5] H. Gross, H. Zügge, M. Peschka, F. Blechinger, "Handbook of Optical Systems", Vol. 3, "Aberration Theory and Correction of Optical Systems", Wiley VCH, Berlin, 600 (2007)
- [6] TIE-25, "Striae in optical glass", http://www.us.schott.com/advanced_optics/download/tie_25_striae_in_optical_glass_2006_us.pdf
- [7] G. S. Settles, "Schlieren and Shadowgraph Techniques", Springer, Berlin (2001)
- [8] B. Zakharin, J. Stricker, "Schlieren systems with coherent illumination for quantitative measurements", Appl. Opt. 43, 4786 (2004)
- [9] J. S. Stroud, "Striae quality grades for optical glass", Opt. Eng. 42, 1618 (2003)
- [10] R. Hild, G. Nietzsche, J. Hebenstreit, "Influence of schlieren on imaging properties of an optical system. II: Modulation Transfer Function (MTF)", Optik 85, 177 (1990)
- [11] R. Hild, S. Kessler, G. Nietzsche, "Influence of schlieren on imaging properties of an optical system. I: Point spread function (PSF)", Optik 85, 123 (1990)
- [12] H. Köhler, "Der Einfluß von Glasschlieren auf die Güte der optischen Abbildung", Optik 21, 339 (1964)
- [13] H. Köhler, R. Keller, "Kontrastübertragungsfunktion einer optischen Abbildung, die durch Rechteckschlieren gestört ist", Optik 21, 372 (1964)
- [14] V. S. Doladugina, "Evaluating the stria content in optical glass", J. Opt. Technol., 71, 836 (2004)
- [15] W. Singer, M. Totzeck, H. Gross, "Handbook of Optical Systems", Vol. 2, "Physical Image Formation", Wiley VCH, Berlin, (2005)
- [16] I. Nunez, J. A. Ferrari, "Bright versus dark schlieren imaging: quantitative analysis of quasi-sinusoidal phase objects", Appl. Opt. 46, 725 (2007)